Available online at www.sciencedirect.com
SCIENCE DIRECT®
Journal of Chromatography A, 1069 (2005) 113–118
JOURNAL OF CHROMATOGRAPHY A
www.elsevier.com/locate/chroma

Short communication

Applicability of the stoichiometric displacement model to description of the retention behavior of charged-fusion proteins during fast protein liquid chromatography

Chenming Zhang [a,*], Charles E. Glatz [b]

[a] *Department of Biological Systems Engineering, Virginia Polytechnic Institute and State University, Blacksburg, VA 24061, USA*
[b] *Department of Chemical Engineering, Iowa State University, Ames, IA 50011, USA*

Abstract

The applicability of the stoichiometric displacement model (SDM) to description of the retention behavior of charged-fusion proteins in large ion exchange resin (~90 μm diameter) packed column was studied. Proteins were characterized by SDM for isocratic elution. The parameters were subsequently used to evaluate their suitability in predicting protein retention and peak width under gradient elution. The proteins were β-glucuronidase (GUS) and its fusions with polypeptides of 5, 10 and 15 aspartic acids at the C-terminal of the wild-type GUS. Predictions of retention time were within 10% of the experiment results. The plate number obtained at high salt concentration from isocratic elution was used as a first estimate for predictions of peak width. The results show that the SDM is sufficient to describe the binding equilibrium of fusion proteins in ion-exchange columns packed with large resin particles. In addition, the binding mechanism between fusion proteins and the ion exchanger is explored with the assistance of comparative molecular modeling.

Keywords: Ion-exchange chromatography; Fusion protein; Protein retention; Glucuronidase; FPLC; SDM

1. Introduction

Ion-exchange chromatography (IEC) is widely used in separation and fractionation of proteins [1,2]. It is most effective when there are sufficient charge differences among the proteins to be separated. Recombinant DNA technology permits alteration of protein charge to provide for charge differentiation, and fusions of charged amino acids to proteins have been used as a separation strategy for both microbial [3] and plant systems [4,5].

The stoichiometric displacement model (SDM) was introduced to describe protein binding equilibrium on ion-exchange chromatography by Regnier and coworkers [6–9] based on the work by Boardman and Partridge [10]. In the SDM, the equilibrium is between the competitive binding of protein and a stoichiometric number of counterions. The same form of binding expression was applied to gradient elution to provide an expression to predict the elution of a protein from known binding equilibrium parameters [11].

The SDM was joined to fusion technology in characterization of a series of β-galactosidase/polyaspartate fusions on anion-exchange chromatography [12]. In that case, fusions were thought to enhance binding by a combination of an increased charge footprint and reduced dissociation rate because of the multipoint attachments. Their work showed that charged fusions could serve as the dominant "footprint" whereas for point mutations [13], the contribution of added charge depended on location. However, the mechanism of fusion tails interacting with the stationary phase has not been explored in detail, and no effort was made to extend the use of the equilibrium expressions beyond the mode of isocratic elution to describe fusion proteins' retention. Here we report the application of the SDM in characterization of the equilibrium binding of a series of β-glucuronidase fusions with different lengths of polyaspartate fusions and the use of the information in predicting gradient elution of these proteins during fast protein liquid chromatography (FPLC). We also

* Corresponding author. Tel.: +1 540 231 7601; fax: +1 540 231 3199.
E-mail address: cmzhang@vt.edu (C. Zhang).

0021-9673/$ – see front matter © 2005 Elsevier B.V. All rights reserved.
doi:10.1016/j.chroma.2005.02.041

attempt to illustrate the protein–resin interaction mechanism with the assistance of molecular modeling.

2. Theoretical framework

The stoichiometric displacement model [6,8,9] characterizes an ion-exchange process as

$$P_0 + ZC_b \Leftrightarrow P_b + ZC_0 \quad (1)$$

where P_0 and P_b refer to protein concentration in the mobile and stationary phases, respectively; C_b and C_0 refer to the concentration of the bound and free salt ion; and Z is the number of bound ions displaced during the protein adsorption process. The protein retention (the retention factor k) can be related to the displacing ion concentration in mobile phase by

$$\log k = \log I + Z \log (C_0)^{-1} \quad (2)$$

where $k = (t_R - t_{NR})/t_{NR}$, and t_R and t_{NR} are the retention times of the solute at retained and non-retained conditions, respectively. I is a protein-specific constant, which indicates the overall (specific and non-specific interactions) affinity of the solute for the sorbent surface [13]. Eq. (2) can be used to obtain the two protein-specific parameters, Z and I, by plotting k obtained from at a series of isocratic elution conditions (C_0).

In linear gradient elution, the displacing ion concentration, $C_{0(g)}$, at which a protein elutes can be calculated from the derivation by Jandera and Churacek [11].

$$C_{0(g)} = \left[G(Z+1)IV_m + C_{0,e}^{Z+1}\right]^{1/Z+1} - GV_d \quad (3)$$

where $C_{0,e}$ is the eluent salt concentration at the start of the gradient; V_m is the total volume of the mobile phase in the column; V_d is the dead volume of the connection tube between the outlet of the gradient generating device and the top of the column; and G is the gradient slope in mobile phase volume scale (mM/mL). Z and I are protein-specific parameters obtained from the SDM. The peak width in gradient elution, w_g, can be related to that (w) observed where elution is carried out isocratically at the concentration where elution occurs in gradient mode by

$$w_{(g)} \approx w = \frac{4V_R}{\sqrt{N}} = \frac{4V_m}{\sqrt{N}}(IC_{0(g)}^{-Z} + 1) \quad (4)$$

Neglecting axial diffusion, the plate number is obtained ($N = L/H$ where L is the bed height, and H can be correlated according to the van Deemter equation) through the height equivalent to a theoretical plate, H, as a function of the chromatographic (i.e. interstitial) velocity, u (=FL/V_m) [14,15]

$$H = A + Cu \quad (5)$$

where F is the volumetric flow rate. Constant A (=$2\lambda d_p$, where λ is a packing characterization factor, and d_p is the particle diameter) represents the contribution of nonuniformity of linear velocity in the mobile phase at the cross section of a column (eddy diffusion), and C accounts for exchange kinetics between resin and fluid—internal and external mass transfer.

3. Materials and methods

3.1. Materials

Sodium monobasic phosphate, sodium dibasic phosphate, and sodium chloride were purchased from Fisher (Itasca, IL). The econo-column was purchased from Bio-Rad (Hercules, CA). Q-sepharose fast flow resin (average particle size of 90 μm), BSA standard, and other chemicals were purchased from Sigma (St. Louis, MO).

3.2. GUS and its fusions

β-Glucuronidase (GUS) of *E. coli* is very stable and has a p*I* of about 5.5. The active protein is a tetramer, and each monomer has a molecular mass of ∼68 000 [16]. Three fusions were developed based on the wild-type GUS, and they are designated as GUSD0 (wild-type) and GUSD5, GUSD10, and GUSD15, according to the number of aspartates fused to the carboxyl terminus. The expression and purification of wild-type GUS and its variants can be found elsewhere [5]. The GUS assay is based on the protein's ability to hydrolyze *p*-nitrophenyl β-D-glucosiduronic acid (PNPG) to release chromophore *p*-nitrophenol [17,18], and GUS activity is expressed as unit/mL. One unit of GUS can liberate 1 nmol *p*-nitrophenol/min from PNPG at 37 °C and pH 7.0 [5].

3.3. Chromatography

The strong anion exchanger, Q-Sepharose fast flow (bead average diameter ∼ 90 μm), was packed into a 15 cm × 1 cm I.D. empty econo-column to a final height of 6.7 cm (5.26 mL). Chromatographic experiments were carried out using an FPLC system controlled by BioLogic software (Bio-Rad, Hercules, CA). The equilibrating buffer used was 50 mM sodium phosphate (NaPi) pH 7.0 (buffer A), while the high salt elution buffer was 50 mM NaPi, 1 M NaCl, pH 7.0 (buffer B). Flow rate was 1 mL/min for gradient elution experiments, and the columns were operated under a pressure of ∼20 psi. Fractions of the column effluent were collected and assayed to identify the GUS peak. All experiments were repeated at least twice.

3.4. System parameters

The dead volume from the outlet of the gradient generation device to the top of the bed, V_d, was determined by directly measuring the volume of the connection tubing. V_d = 0.61 mL.

The column total porosity was determined from the retention time by injecting a pulse of acetone in buffer A (0.1 mL, 10%, v/v) into the column, followed by elution at 0.1 mL/min with 50 mM NaPi, pH 7.0, and monitoring the column effluent at 280 nm [19]. $\varepsilon = 0.903$.

The bed ion capacity, Λ, was determined by frontal analysis [20]. The column was first equilibrated by 50 mM Tris–HCl, pH 7.0. A front of sodium nitrate (repeated for concentrations ranging from 50 to 300 mM) in 50 mM Tris–HCl, pH 7.0, was then introduced at 1 mL/min, and the eluent was monitored at 280 nm. The capacity was determined from the nitrate breakthrough front, and $\Lambda = 201$ mM.

The plate number ($N = L/H$) for each fusion protein was obtained by correlating (Eq. (5)) relationship between the plate height and the chromatographic velocity to the flow rate used in gradient elution experiments. The correlation was obtained based on a series of isocratic elution experiments when proteins are at non-retained conditions (with 2 M NaCl in the protein samples). The flow rates were low enough to yield symmetric elution peaks, and the injection volume was 100 μL.

4. Results and discussion

4.1. Protein parameters, Z and I, in SDM, and fusion protein binding mechanism

The SDM parameters for each protein were determined by measurement of the retention factors, k, for a series of isocratic elution experiments carried out at different salt concentrations, C_0, and plotting the results according to Eq. (2) (Fig. 1). The 50 mM phosphate anion in the equilibrating buffer was treated as equivalent to an additional 50 mM of chloride anion. Values of characteristic charge (Z) and the solute specific parameter (I) from such plots, along with the estimated protein net charges at neutral pH are summarized in Table 1.

The characteristic charge of GUS increases four units for each additional five aspartates added in the series of tails for GUSD0, GUSD5, and GUSD10. By a comparative modeling using human β-GUS (a dimeric protein whose monomer shares 45% amino acid identity with *E. coli* β-GUS monomer) as a template (data not shown), one possible explanation is that the presence of the fusion tails redirects the orientation of the protein during its interaction with the ion exchange resin to take advantage of multipoint binding. The result is that two out of the four fusion tails participate in the protein's retention while each of the two tails contributing three binding sites for GUSD5 and five for GUSD10 while giving up two distributed sites on GUSD0 due to the reorientation. This will thus account for the increase of Z value from 8.3 for GUSD0 to 12.2 for GUSD5 and further to 16.1 for GUSD10. This also indicates that the fusion tails dominate the protein–resin interaction, and the multipoint attachment at the "footprint" limits the spatial flexibility of the protein thus the involvement of all tails and other binding sites on the protein in the interaction. Moreover, the data indicate that the extension of tail length is efficient when the number of aspartates is less than 10. K_{eq} and overall affinity, I, increase along with Z, and the increment is directly proportional to the length of the fusion tail. Heng and Glatz [12] reported a similar but smaller increment in Z for the tetrameric β-galactosidase.

Table 1
Nominal protein charge and stoichiometric displacement model binding parameters

Protein	Estimated net charge	Characteristic charge, Z	Protein parameter, I
GUSD0	−75	8.3	5.2×10^{20}
GUSD5	−95	12.2	1.5×10^{32}
GUSD10	−115	16.1	3.3×10^{43}
GUSD15	−135	12.1	5.1×10^{32}

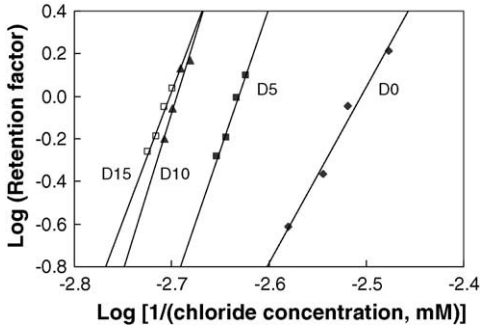

Fig. 1. Plot of log(retention factor) vs. log(chloride concentration) for isocratic elution of GUS and its fusions. The protein names have been abbreviated as D0, D5, D10, and D15, respectively.

However, the increment from 10 to 15 aspartates on the tails results in not only a smaller Z, but also a smaller equilibrium constant and overall affinity. The decreased effectiveness of binding behavior of the longer-tailed GUSD15 is consistent with previously reported work done on β-galactosidase fusions [12,21]. This may be caused by either an interaction of the tail with the core GUS or some secondary structure formed within the longest fusion as has been proposed for oligonucleotides [8]. By performing energy minimization with molecular modeling on GUSD15, neither interaction between the fusion tail and the protein body nor the formation of secondary structure in the tail seemed to be energy favored. However, since human β-GUS was used in the modeling, none of the possibilities could be affirmatively excluded. It is certain, however, that when using fusion technology to enhance protein purification, the selection of the tail length is critical, and longer tails do not necessarily improve protein binding and separation.

4.2. Number of theoretical plates, N

The plate height as a function of chromatographic velocity is shown in Fig. 2. It can be seen that all data are fitted extremely well by Eq. (5) in the range of flow rates used

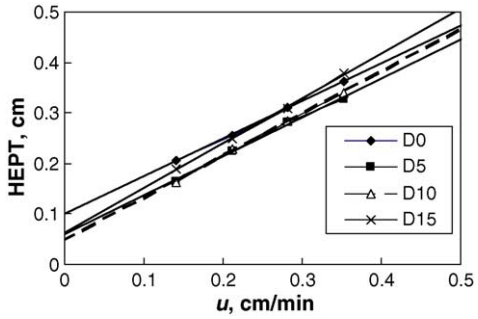

Fig. 2. Plot of HETP vs. the chromatographic velocity, $u = FL/V_m$, for GUS and its fusions. Where L is the bed height, $V_m = \varepsilon \times$ total bed volume, and F is the volumetric flow velocity in mL/min. Equilibrating buffer and sample carrier buffer was 50 mM NaPi, 2 M NaCl, pH 7.0; injection volume = 100 μL.

in the isocratic experiments. However, to obtain the plate number for the estimation of the peak width during gradient elution (Eq. (4)), the plate height relationship with u needs to be extended to the flow rate used for the gradient elution experiments, 1 mL/min. The results of the fitted equation between HETP and u, and the extrapolation results are included in Table 2. Due to the low number of plates, the plate height at 1 mL/min may also be calculated using Knox equation [22], $h = A\nu^{1/3} + C\nu$, where h is reduced plate height (=HETP/d_p), and ν is reduced velocity (=$d_p u/D_m$). D_m is the protein molecular diffusivity, and for proteins with molecular mass of MM at temperature T, it can be estimated by, $D_m = 8.34 \times 10^{-8} MM^{-1/3} \eta T$ [23]. For GUS and its fusions at 293 K in a packed column using ~90 μm resins, $D_m = 0.37 \times 10^{-6}$ cm^2/s. The plate heights and numbers obtained by Knox equation are also included in Table 2. The plate numbers by Knox equation are slightly higher than that obtained by van Deemter equation, but the differences are not significant enough to affect the trends in the comparison of the experimentally obtained and calculated peak widths shown in the next section.

4.3. Protein elution and prediction

Linear gradient experiments with four different gradient slopes were carried out in order to examine the ability of Eqs. (3) and (4) to capture the effect of changing elution conditions. All protein elution peaks were identified by activity assays on collected fractions, because UV absorbance was not sufficient for identification of the GUS peaks. The activity peaks of the four GUS proteins under same gradient elution are superimposed in the same chromatogram in Fig. 3. While increasing the gradient slope understandably diminishes the impact of the fusions on elution time, the differences in salt concentration at which they elute remain relatively constant (Fig. 3).

Also shown in Table 3 is the prediction for salt concentration at which elution will occur during gradient elution, calculated from Eq. (3) and the values of Z and I from Table 1. In most cases, the model predicts the protein peak elution reasonably well with an error of less than 10%. The primary source of error could come from the estimation of Z and I values, especially Z value. As expected, Eq. (3) is very sensitive to Z. A 1% change of Z value will result in 5% change in the predicted salt concentration for peak elution, and meanwhile, 1% change of I will only cause the predicted peak elution to change ~0.1%. Therefore, obtaining accurate Z values is crucial for accurate prediction of the peak elution. For GUSD0, because of the presence of an overlapping *E. coli* peak made determination of isocratic elution times (and, therefore, Z and I) more difficult, unsurprisingly, the prediction of the elution times has the largest errors. In addition, the fact that the protein elution peaks had to be determined by activity assays of finite fractions also contributes an error of ~2%.

Compared with the elution predictions of non-fusion proteins using the same method on HPLC (particle size, 7 μm) [24], where the predicted values are within ±1% of the experiment results, the errors of fusion proteins are slightly larger. However, the difference could solely come from the experimental errors in obtaining the peak positions and Z values. Herein, it is demonstrated that the stoichiometric displacement model is sufficient to describe protein binding equilibrium in ion-exchange columns packed with large resin particles.

The experimental and predicted peak widths are also shown in Table 3. The plate numbers obtained by van Deemter equation are used in the calculation of the peak widths. In general, the predicted peak widths are in good agreement with the experimental results, but some errors are greater than 30%. Similar to the predictions of peak elution, Z value has a great effect on the predictions of the peak width using Eq. (4), meanwhile the equation is not sensitive to the variation of I value. In addition, another very important factor for the significant deviation probably comes from the necessity of constructing the protein elution peaks from assays on fractions collected during the experiments. The fraction size, 0.63 in

Table 2
Estimation of plate number at 1 mL/min based on Eq. (5)

Protein	HETP vs. u	HETP at 1 mL/min cm	N at 1 mL/min	HETP[a]	N[a]
GUSD0	HETP = 0.745u + 0.1	1.15	5.8	1.02	6.6
GUSD5	HETP = 0.769u + 0.059	1.14	5.9	1.07	6.5
GUSD10	HETP = 0.834u + 0.048	1.22	5.5	1.16	5.8
GUSD15	HETP = 0.887u + 0.063	1.31	5.3	1.24	5.4

Bed height = 6.7 cm.
[a] Results obtained using $h = A\nu^{1/3} + C\nu$ to fit the data.

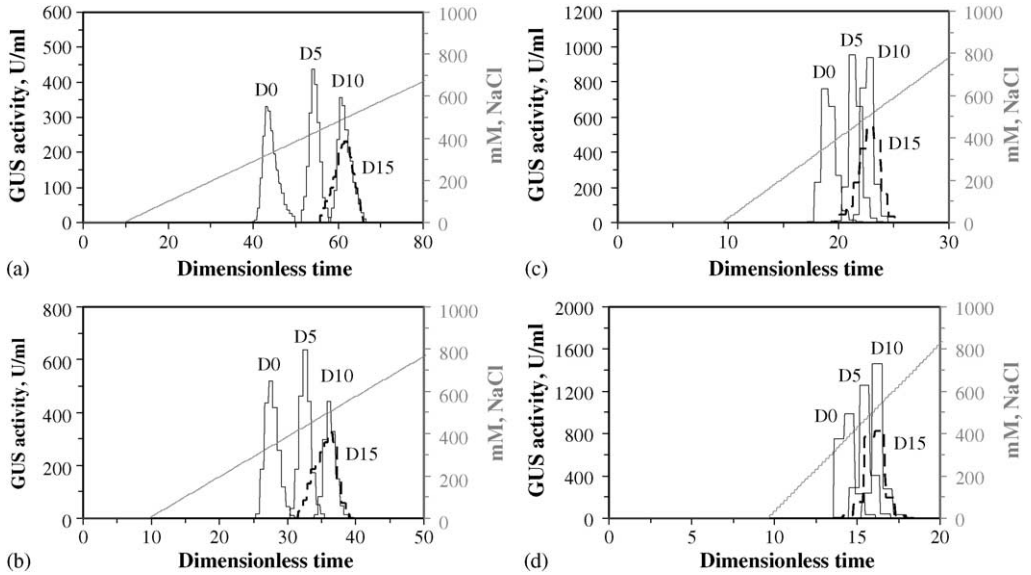

Fig. 3. Superpositioning of the normalized GUS activity peaks from individual chromatographic runs of the series of GUS fusions with linear gradient elution. Feed injection: 250 μl of sample in 50 mM NaPi, pH 7.0. After washing with equilibrating buffer (50 mM NaPi, pH 7.0), a linear NaCl gradient was introduced into the column. Operating conditions: 1 mL/min, pH 7.0, 3 mL fractions collected for assay. Gradient slopes (mM/mL): (a) 2; (b) 4; (c) 8; (d) 16.7. All activity peaks shown were normalized to a peak area corresponding to 100% GUS recovery. Dimensionless time = t/t_0, where t is the elution time and t_0 is the time needed for the mobile phase to pass through the total void volume in the bed.

Table 3
Experimental and predicted protein retention (by Eq. (3)) and peak width (by Eq. (4))

Protein	Gradient slope, G (mM/mL)	Protein retention			Peak width		
		Experiment results, $C_{0(g)}$ (mM)	Predicted results, $C_{0(g)}$ (mM)	Error (%)	Experiment results, $w'_{(g)}$	Predicted results, $w'_{(g)}$	Error (%)
GUSD0	2	320	277	13	10.0	6.2	38
	4	341	298	13	5.7	4.2	27
	8	353	319	10	5.0	3.1	38
	16.7	395	340	14	3.1	2.5	19
GUSD5	2	424	389	8	6.9	7.8	−13
	4	436	409	6	5.0	5.0	0
	8	447	429	4	4.3	3.5	18
	16.7	464	448	3	3.1	2.8	11
GUSD10	2	487	465	5	8.8	8.1	8
	4	502	483	4	4.9	5.2	−5
	8	510	500	2	3.0	3.6	−22
	16.7	521	517	1	2.5	2.8	−14
GUSD15	2	497	451	9	10.0	8.5	15
	4	507	475	6	7.5	5.4	28
	8	510	498	2	5.6	3.8	32
	16.7	532	522	2	3.8	2.9	23

dimensionless time, can contribute greatly to the determination of the actual peak width. The experimental error caused by fraction collection varies from 6% to 25% (6% when peak width is 10, and 25% when peak width is 2.5). However, this error could be reduced by collecting smaller fractions.

The peak widths for GUSD15 are noticeably greater than for the other proteins (Fig. 3). Whether or not the model used here has captured this effect through the Z and I values is difficult to evaluate because of the error associated with the fraction size. The protein conformational change due to the mobile phase composition change during gradient elution could also have serious effect on peak shape and width [25]. This appears to be the case especially for GUSD15.

5. Conclusions

Fusion lengths of up to 10 aspartates significantly improved binding of β-glucuronidase to anion exchange resins—the equilibrium constant increased by a factor of 220.

The binding of the fusion proteins conformed to the SDM model and the resulting values of *Z* and *I* provide insight into the contribution of the fusion. Under studied loading conditions, the SDM parameters could be used to give reasonable predictions for protein retention and peak width over a range of gradient conditions on FPLC columns. A better test of the peak prediction, especially the width, could have been obtained by collecting much smaller fractions during the experiments.

From the comparative modeling using human β-GUS as a template, it is highly likely that two of the four fusions tails participate in protein–resin interaction with each tail contributing three and five effective binding sites for GUSD5 and GUSD10, respectively, meanwhile two distributed binding sites on GUSD0 are lost due to the protein reorientation. Also, the presence of fusion tails dominates the binding thus preventing all the distributed binding sites on protein (GUSD0) from interacting with the ion exchangers. Fusion proteins with long polypeptide tail (GUSD15) behave differently from those having shorter tails. It indicates that it is important to select the appropriate length of fusion tail to enhance a protein's binding in ion-exchange chromatography.

Acknowledgments

This material is based upon work supported by the National Science Foundation under Grant No. BES9522644. The authors thank ProdiGene Inc., College Station, TX, for providing *E. coli* strains encoded with GUS and its fusions. We also thank Mr. Lakshmi Pathange, a graduate student in Dr. Zhang's laboratory, for providing assistance in molecular modeling.

References

[1] J. Bonnerjea, S. Oh, M. Hoare, P. Dunnill, Bio/Technology 4 (1986) 954.
[2] C.J.O.R. Morris, P. Morris, Separation Methods in Biochemistry, second ed., Pitman, London, 1976.
[3] H.M. Sassenfeld, S.J. Brewer, Bio/Technology 2 (1984) 76.
[4] C.-M. Zhang, C.E. Glatz, Biotechnol. Prog. 15 (1999) 12.
[5] C.-M. Zhang, R.T. Love, J.M. Jilka, C.E. Glatz, Biotechnol. Prog. 17 (2001) 161.
[6] W. Kopaciewicz, M.A. Rounds, J. Fausnaugh, F.E. Regnier, J. Chromatogr. 266 (1983) 3.
[7] M.A. Rounds, F.E. Regnier, J. Chromatogr. 283 (1984) 37.
[8] R.R. Drager, F.E. Regnier, J. Chromatogr. 359 (1986) 147.
[9] R.R. Drager, F.E. Regnier, J. Chromatogr. 406 (1987) 237.
[10] N.K. Boardman, S.M. Partridge, Biochem. J. 59 (1955) 543.
[11] P. Jandera, J. Churacek, J. Chromatogr. 91 (1974) 223.
[12] M.H. Heng, C.E. Glatz, J. Chromatogr. A 689 (1995) 227.
[13] R.M. Chicz, F.E. Regnier, Anal. Chem. 61 (1989) 2059.
[14] S. Yamamoto, K. Nakanishi, R. Matsuno, Ion-exchange Chromatography of Proteins, Marcel Dekker Inc., New York, NY, 1988.
[15] F.H. Arnold, H.W. Blanch, C.R. Wilke, J. Chromatogr. 330 (1985) 159.
[16] R.A. Jefferson, S.M. Burgress, D. Hirsh, Proc. Natl. Acad. Sci. U.S.A. 83 (1986) 8447.
[17] K. Kato, K. Yoshida, H. Tsukamoto, M. Nobunaga, T. Masuya, T. Sawada, Chem. Pharm. Bull. 8 (1960) 239.
[18] R.A. Jefferson, K.J. Wilson, Plant Mol. Biol. Manual B14 (1991) 1.
[19] S.U. Kim, J.A. Berninger, Q. Yu, N.-H.L. Wang, Ind. Eng. Chem. Res. 31 (1992) 1717.
[20] S.D. Gadam, G. Jayaraman, S.M. Cramer, J. Chromatogr. 630 (1993) 37.
[21] M.Q. Niederauer, I. Suominen, M.A. Rougvie, C.F. Ford, C.E. Glatz, Biotechnol. Prog. 10 (1994) 237.
[22] J.H. Knox, H.P. Scott, J. Chromatogr. 282 (1983) 297.
[23] M.E. Young, P.A. Carroad, R.L. Bell, Biotechnol. Bioeng. 22 (1980) 947.
[24] E.S. Patente, D.B. Wetlaufer, J. Chromatogr. 355 (1986) 29.
[25] L.R. Snyder, J.W. Dolan, Adv. Chromatogr. 38 (1998) 115.